Wavelength Dependence of Photooxidation vs Photofragmentation of Chromocene

Peter T. Muraoka, Daniel Byun, and Jeffrey I. Zink*

Department of Chemistry and Biochemistry, University of California, Los Angeles, California 90095

Photooxidation and metal−ligand photolysis reactions of bis(cyclopentadienyl)chromium, chromocene, in the range 24 390−15 630 cm^{-1} are studied in the gas phase by using time-of-flight mass spectroscopic detection. Photooxidation of the intact chromocene molecule unexpectedly dominates in the range 23 530−24 000 cm^{-1}. The relative importance of photooxidation compared to photofragmentation is strongly wavelength dependent. A prominent species at all wavelengths is the chromium ion, but in a wavelength region corresponding to the lowest energy ligand to metal charge transfer excited electronic state absorption, the strongest peak is from the chromocene ion. The excitation spectra are reported for three selected species: chromocene ion, mono-(cyclopentadienyl)chromium ion, and the chromium ion. The spectrum obtained by monitoring the metal ion contains sharp peaks that are assigned to neutral chromium atom resonances. Sharp losses of intensities in the molecular ion spectra are observed at these wavelengths. The wavelength dependencies of the photoreactions are interpreted and explained in terms of the identity of the initially populated excited electronic state and the ionization energy of the molecule. When the initially populated excited electronic state is the ligand to metal charge transfer state, the first photon causes minimal bond weakening and the second photon excites the intact chromocene above the ionization energy, resulting in efficient ionization of the parent molecule. When the initially populated state is a lower energy ligand field excited electronic state, bond weakening occurs and absorption of a second photon results in significant photodissociation producing intense fragment peaks dominated by the metal ion peak.

Introduction

The gas phase photochemical reactions of metal compounds, and especially the primary photochemical processes such as photodissociation and photofragmentation, are attracting interest because of their importance in understanding laser assisted chemical vapor deposition.[1−5] Identification and quantification of the photofragments use luminescence spectroscopy and mass spectroscopy as the primary analytical methods.[6−10] Our interest in the photochemistry was sparked by our observations that both desired photofragments (i.e., those having the stoichiometry of the desired deposit) and undesired species (i.e., those that lead to contamination of the desired deposit) are produced by intramolecular processes in the gas phase.[11−13] The amounts of the photofragments that are produced depend on both the wavelength and the fluence of the exciting light. In our studies of chromium metal deposition using tris(hexafluoroacetyl-acetonate)chromium, Cr(hfac)$_3$, as the precursor, we discovered that chromium atoms are readily formed by photolysis but that significant amounts of the undesired diatomic photofragment CrF were also produced intramolecularly.[14,15] To avoid fluorine contamination of the deposit, we investigated other chromium precursors including chromocene, bis(cyclopentadienyl)chromium, Cr(Cp)$_2$.

Multiphoton dissociation of many metallocene compounds has been studied by mass spectroscopy.[16−27] The wavelength dependence of the total ion current spectrum for ferrocene and cobaltocene in the ranges 366−370, 380−390, and 445−455 nm and for nickelocene in the range 375−520 nm was reported.[20,24,25] The features in the excitation spectrum were attributed solely to the metal ion. "Explosive" dissociation directly to the metal was the most commonly observed photolytic pathway. In studies of ferrocene in the UV/vis region,

no ferrocene cations were detected.[17,19−21,24,25] However, in the VUV at 193 nm excitation, the parent ion is observed.[16,26,27] Similar results were reported for nickelocene. The largest reported ratio of parent ion to metal ion intensities in multiphoton ionization of a metallocene was 0.005:1 for nickelocene.[21] The only reported multiphoton dissociation/ionization studies of chromocene employed emission spectroscopy to detect the excited-state photoproducts after excitation at 248 nm.[28] Only emission from atomic Cr was detected.

In this paper, we report the surprising discovery that chromocene ion can be the major product of gas-phase photolysis and that the ratio of chromocene ion to the chromium Cr$^+$ ion is strongly wavelength dependent. We examine this result by using time-of-flight mass spectroscopy and resonance enhanced multiphoton ionization (REMPI) spectroscopy. Excitation within a narrow wavelength range results in photooxidation to produce the molecular ion and fragmentation that includes formation of the monoligated chromium species, the cyclopentadienyl ion, the chromium ion, and small carbon fragments of the ligand. Outside of this wavelength range, complete metal−ligand photolysis occurs and the dominant mass signal is Cr$^+$. Both broad bands and sharp lines in the mass-selected excitation spectra are observed. The wavelength regions that lead to specific fragments are correlated to absorption bands of chromocene and the fragmentation patterns are interpreted in terms of the bonding changes that occur in the initially populated excited state. The sharp lines arise from neutral chromium atom absorption bands.

Experimental Section

The TOF mass spectrometer was constructed based on a design in the literature.[29,30] The chromocene (Aldrich, 95%) is

admitted to the high-vacuum chamber via a supersonic jet. The base pressure of the chamber is less than 10^{-6} Torr. The photoionization for mass spectroscopy is carried out in a stainless steel cube (30 cm edge length) with quartz windows evacuated to 10^{-6} Torr with a 12 in. diffusion pump fitted with a water-cooled baffle. The sample is sublimed at 85 °C before it is seeded in He with a backing pressure of about 10^3 Torr. A General Valve series 9 high-speed solenoid valve (0.5 mm orifice) sends a 0.2 ms pulse of the sample into the chamber to intersect the incoming photons at 90°. An optical parametric oscillator pumped by the third harmonic of a Nd:YAG laser produces the photons within the 24 390−15 630 cm^{-1} range (∼20 mJ/pulse, 10−20 cm^{-1} line width) used for excitation. The laser fluence was only varied in our power dependence studies. The energy range is scanned with a stepping motor driven micrometer that tunes the crystal of the OPO. The wavelength of the OPO output is calibrated with a monochromator and a CCD detector. The total experimental uncertainty in the reported photon energies is ±10 cm^{-1}.

The fragment ions are accelerated down a 1m flight tube by a series of three stainless steel plates that have stainless steel mesh across an open center. Acceleration plate voltages are 3000 V, 2100 V, and ground, respectively, in order from furthest to nearest the detector. The flight tube is kept at 10^{-6} Torr using a Varian V300HT 6 in. air-cooled turbomolecular pump, and ions are detected using an 18 mm microchannel plate detector assembly. The detector assembly is fitted with two Galileo MCP 18B plates with a 10 μm channel diameter and a channel spacing of 12.5 μm. The ion current is processed using a computer-controlled RTD710 Tektronix 200 MHz dual-channel digitizer. A variable delay Stanford Research Systems model SR250 Gated Integrator and Boxcar Averager Module is used for the wavelength dependence studies.

Results

1. Mass Spectra. *a. General Trends and Observations.* A strong feature that is common to all of the mass spectra at all of the wavelengths used for fragmentation and ionization is the group of peaks arising from Cr$^+$. The peaks are observed at 50, 52, 53, and 54 *m/z* and correspond to the most abundant isotopes of chromium. When maximizing the intensity of the minor fragments, the intensities of the dominant Cr$^+$ and Cr(Cp)$_2^+$ become saturated. Mass spectra taken at three representative wavelengths are shown in Figure 1.

The relative intensities of the peaks in the mass spectrum are very wavelength dependent. At photon energies less than about 23 530 cm^{-1}, the peaks from Cr$^+$ dominate the spectrum; all other peaks are less than 1/12 as intense. In the wavelength region between 21 000 and 23 530 cm^{-1}, the peaks from Cr$^+$ are the most intense but peaks from the parent ion and Cr(Cp)$^+$ appear with intensities about 6% that of the metal ion. In the energy region from 23 530 to 24 390 cm^{-1} (the limit of the scanning range of the instrument), the intensity of the parent ion peak is about the same as that of the metal ion. At an energy of 28 170 cm^{-1} (the third harmonic of the Nd:YAG laser), the Cr$^+$ peaks again dominate the mass spectrum and the next most intense peaks arise from C$_1^+$, C$_2^+$, and C$_3^+$ fragments of the ligands with intensities roughly 1/4 to 1/3 that of the metal ion. Representative mass spectra obtained by exciting chromocene at specific wavelengths within these regions are shown in Figure 1 and are described in detail below.

b. 21 170 cm^{-1} (472 nm) Excitation. Figure 1a is representative of the spectra obtained in the 21 000−23 530 cm^{-1} region. The mass spectra obtained at energies lower than 21 000 cm^{-1}
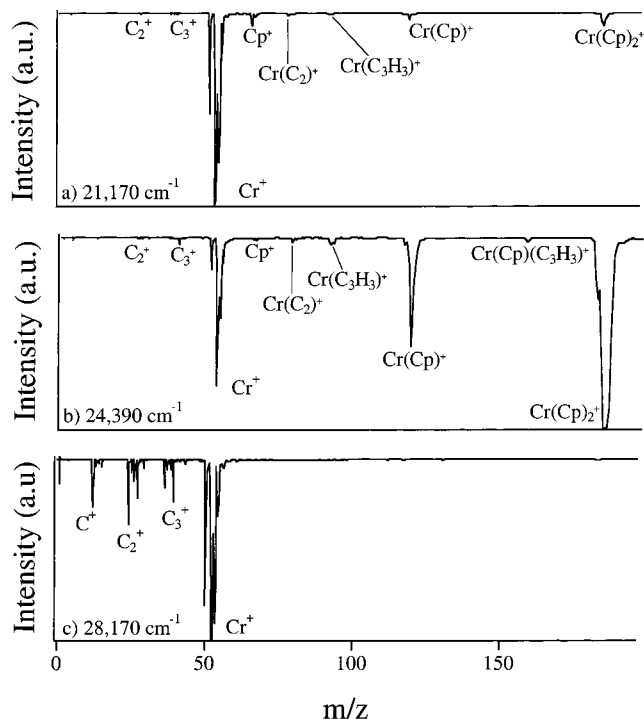

Figure 1. Mass spectra resulting from photolysis of chromocene at (a) 21 170 cm^{-1}, (b) 24 390 cm^{-1}, and (c) 28 170 cm^{-1}. The three peaks appearing at 50, 52, and 53 *m/z* correspond to the isotopes of chromium.

outside this scan region are dominated mostly by Cr$^+$ and fragments of the Cp group, whereas Cr(Cp)$_2^+$ is observed at <1/15 the intensity of the metal ion. However, numerous chromium-containing molecular species, including Cr(Cp)$_2^+$ and Cr(Cp)$^+$ begin to appear in the scan to higher energies in the region 21 000−23 530 cm^{-1}. The appearance of other metal-containing fragments including CrC$_2^+$ and CrC$_3$H$_3^+$ is also evident although the spectra are still dominated by Cr$^+$. At the highest energy region within this scanning range, the molecular peak intensities increase in intensity and never decrease to the intensities observed at lower energies.

c. 24 390 cm^{-1} (410 nm) Excitation. Figure 1b is representative of the spectra in the region 23 530−24 390 cm^{-1}. This fragmentation pattern is unexpected because the chromium-containing molecular species Cr(Cp)$_2^+$ and Cr(Cp)$^+$ have intensities comparable to that of the Cr$^+$ ion. A list of the fragment peaks observed and their intensities relative to Cr$^+$ are reported in Table 1. To the best of our knowledge, this spectrum is the first observation of multiphoton ionization of the intact molecule, and other large molecular ion species, to such a large degree. Cr$^+$ is also observed, but unlike mass spectral data obtained from other metallocenes in this energy region, the molecular ion dominates the mass spectrum.

d. 28 170 cm^{-1} (355 nm) Excitation. Figure 1c shows a mass spectrum obtained at a point to higher energy outside the scan region. The spectrum contains fragments of the Cp ring as well as a detectable amount of Cr(Cp)$^+$ but it is dominated by chromium ions; the relative intensities of the next biggest peak (C$_2^+$) is about one-fifth that of chromium. The cyclopentadienyl ligand itself is extensively fragmented. Other fragments are observed and their intensities relative to Cr$^+$ are listed in Table 1. This complete fragmentation to the metal ion is typical of the patterns reported for photolysis of organometallic compounds.

2. Wavelength Dependence of Photolysis by Mass-Selected REMPI Spectroscopy. The intensities of specific mass peaks

Photooxidation vs Photofragmentation of Chromocene

J. Phys. Chem. A, Vol. 105, No. 38, 2001 **8667**

TABLE 1: Mass Peaks Observed during UV and Visible Wavelength Photolysis of Chromocene[a]

ion$^+$	21 170 cm^{-1}	24 390 cm^{-1}	28 170 cm^{-1}
C			17
CH			2
CH$_2$			1
CH$_3$			2
C$_2$			21
C$_2$H			4
C$_2$H$_2$			7
C$_2$H$_3$	<1	<1	12
C$_2$H$_4$			<1
C$_2$H$_5$			3
C$_3$			9
C$_3$H			3
C$_3$H$_2$			3
C$_3$H$_3$	2	5	15
C$_3$H$_4$			<1
C$_3$H$_5$			<1
C$_3$H$_7$			1
Cr	100	100	100
C$_5$H$_5$ (Cp)	8	2	
CrC$_2$	1	3	
CrC$_3$H$_3$	0.6	4.5	
CrCp	3.1	74.0	
CrCpC$_3$H$_3$		2.8	
Cr(Cp)$_2$	6.4	138.1	

[a] The intensities are calculated relative to that of Cr$^+$. All peaks with intensities greater than 0.003 that of Cr$^+$ are listed

are measured as a function of the photon energy in order to obtain more detailed information about the wavelength dependencies. The plots, or REMPI spectra, that are obtained when the Cr$^+$, Cr(Cp)$^+$, and Cr(Cp)$_2$$^+$ ions are monitored are shown in Figure 2.

Chromium Ion. The wavelength dependence of the intensity of Cr$^+$ from chromocene photolysis throughout the 21 500–24 000 cm^{-1} range is shown in Figure 2c. The spectrum is relatively flat between 21 500–22 000 cm^{-1}. As the laser is scanned beyond this range to higher energies, the Cr$^+$ signal increases and the resulting spectrum is full of sharp features. The spectrum has a downward slope between 23 530–24 000 cm^{-1} (425–417 nm) except for the presence of a sharp peak at 23 830 cm^{-1}. For reasons that are discussed later, the sharp peaks are assigned to the ionization of neutral chromium atoms from atomic resonant states.

Cr(Cp)$^+$. The REMPI spectrum obtained by monitoring Cr(Cp)$^+$ in Figure 2b shows a relatively flat nonzero signal in the range 21 500–23 530 cm^{-1}. The Cr(Cp)$^+$ intensity slowly increases as the laser is scanned to higher energies until the onset of a broad band in the 23 530–24 000 cm^{-1} range. The spectrum also shows a sharp dip in the Cr(Cp)$^+$ intensity at 23 830 cm^{-1} along this rising band. This dip is also present in the REMPI spectrum of the intact molecular ion and coincides with a maximum in the Cr$^+$ spectrum.

Cr(Cp)$_2$$^+$. The REMPI spectrum obtained by monitoring Cr(Cp)$_2$$^+$ in Figure 2a shows wavelength-dependent behavior very similar to that of Cr(Cp)$^+$. However, the intensity of the Cr(Cp)$_2$$^+$ signal is about 2 times greater than that of the Cr(Cp)$^+$ ion. At energies lower than 23 530 cm^{-1}, the molecular ion signal intensities are small and relatively constant. The REMPI spectrum of Cr(Cp)$_2$$^+$ also shows a gradual increase in the molecular ion signal between 23 530–24 000 cm^{-1}. A scan in this range traces a broad band characteristic of molecular spectra but at 23 830 cm^{-1} there is a dip in the spectrum that coincides with a maximum in the Cr$^+$ spectra. Comparison of the wavelength-dependent properties of Cr$^+$ and Cr(Cp)$_2$$^+$ will play a major role in the following discussion.
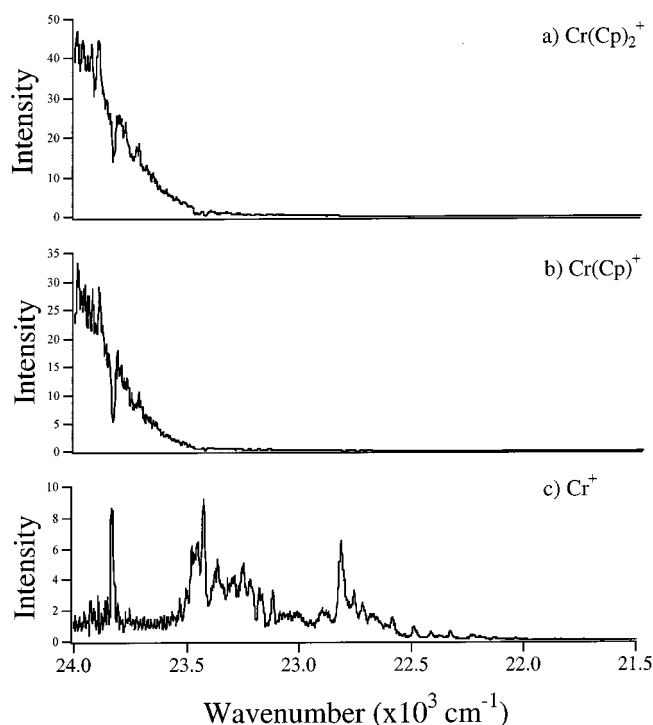

Figure 2. REMPI spectra obtained monitoring (a) Cr(Cp)$_2$$^+$, (b) Cr(Cp)$^+$, and (c) Cr$^+$. Note the different intensity scales.

3. Mass Spectra at Energies Corresponding to Sharp REMPI Peaks. *23 660 vs 23 490 cm^{-1} (423 nm vs 426 nm) Excitation.* Careful comparison of the Cr$^+$ and Cr(Cp)$_2$$^+$ REMPI spectra shows that there are specific wavelengths where a maximum in the Cr$^+$ spectrum has a corresponding minimum in the Cr(Cp)$_2$$^+$ spectrum. The most obvious peak and dip occur at 23 830 cm^{-1}. When the laser is tuned into a sharp peak in the REMPI spectrum, the Cr$^+$ ion signal is so strong that it saturates the ion detector as shown in Figure 3b. When the laser is tuned off of the sharp peak, both the Cr$^+$ and the Cr(Cp)$_2$$^+$ ion signals are of comparable intensity as shown in Figure 3a. The surrounding mass peaks have about the same relative intensities in both cases.

4. Fluence Dependence of Photofragmentation. To study the effect of fluence, mass spectra were taken at varying laser pulse energies. In the 23 500–21 500 cm^{-1} range, the Cr$^+$ intensity decreased more rapidly relative to the intensity of the metal-containing molecular fragments when the laser fluence decreased. The observed photon law was calculated by plotting the log of the intensity of the ion signal vs the log of the laser fluence (Figure 4). A two-photon power law is observed for production of the molecular ion at 21 320 and 24 260 cm^{-1}. A two-photon power law is also observed for production of the chromium ion at energies above ~23 500 cm^{-1}, whereas a four-photon power law is observed at energies below ~23 500 cm^{-1}. Because of saturation effects, more photons than are measured in the experimental photon power law may be involved.[31]

Discussion

1. Mass Spectroscopy. When a molecule is placed in an intense visible or UV laser field, multiphoton absorptions may occur and population of high energy states is possible.[31–37] Molecules placed in this field may continue to absorb photons until the molecule loses its energy by emission, ionization, decomposition or radiationless transition.[32,37] The mechanisms of multiphoton ionization and dissociation have been characterized by two different pathways: ladder climbing and ladder
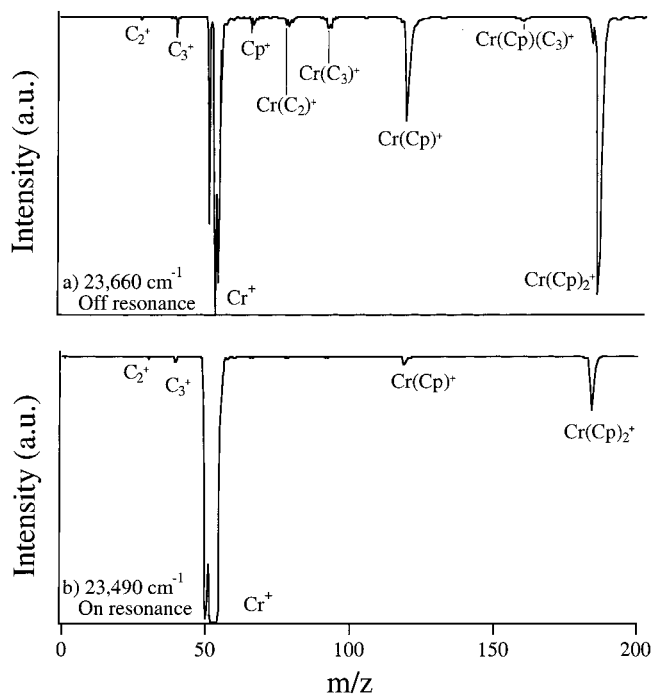
Figure 3. Mass spectra of chromocene a) off resonance (23 660 cm^{-1}) and (b) on resonance (23 490 cm^{-1}). Saturation of the detector at the position of the Cr$^+$ signal can be seen in the bottom spectrum. The peaks labeled as containing carbon species (C$_n^+$) actually contain the range of protonated Cp ring fragments (C$_n$H$_1$)$^+$ to (C$_n$H$_{2n+1}$)$^+$.

switching.[31,37] Each pathway starts with photon absorption that places the molecule (or fragment) in an excited state. The former pathway involves absorption of additional photons until the ionization continuum is reached and parent ions are produced. The latter involves bond breaking before the parent molecule can be ionized; additional photon absorption processes ionize the fragments and the mass spectrum is dominated by fragment ion peaks. Most transition metal compounds possess relatively weak metal−ligand bonds and follow the ladder switching mechanism whereby one or more photons cause metal−ligand bond breaking before the parent molecule is ionized. The metal ion peak dominates the mass spectrum and the parent ion peak is usually very weak or absent.

The relative intensities of the intact chromocene ion in the mass spectra during visible excitation are somewhat surprising. In previous photolytic investigations of many other organo-metallic molecules, the intact molecular ion was rarely seen, and never before with an intensity similar to that of the metal ion.[21] Photon initiated fragmentation studies found in the literature mainly report the observation of the metal ion and low mass fragments of the ligand. In addition to these species, we observe the intact molecular ion as well as other chromium-containing molecular fragments. Table 1 shows the relative intensities of the mass fragments observed during photodissociation of chromocene at 21 170 cm^{-1}, 24 390 cm^{-1}, and 28 170 cm^{-1}. The ratios are determined relative to the most abundant isotope of chromium at 52 *m/z*. Correlations between the photofragmentation and specific spectral regions are discussed below.

Photodissociation at energies lower than 23 530 cm^{-1} produces a fragmentation pattern that is typical of those previously reported for metallocenes,[16−27] i.e., dominated by the metal ion. The occurrence of Cr atomic resonant ionization is predominant and is evidenced by the group of sharp peaks arising from Cr atomic transitions that are observed in the REMPI spectra in

this region. However, other metal-containing species such as Cr(Cp)$^+$, CrC$_2^+$, and CrC$_3$H$_3^+$ are observed but at less than 10% of the intensity of the chromium ion. It is relevant to note that the metal−carbon fragments mentioned above as well as the C$_n^+$ fragments of the Cp ring (C$_2^+$, C$_3^+$, etc.) represent the group of protonated species (C$_n$H$_1$)$^+$ to (C$_n$H$_{2n+1}$)$^+$.

At 21 170 cm^{-1}, the ratio of the monoligated fragment and the molecular ion to that of the metal ion are roughly 0.03:1 and 0.06:1, respectively. The favored mechanism in this region most likely involves photodissociation of chromocene before it is excited above the ionization continuum. The spectra in this region are characteristic of those observed in other metallocenes as there is a very intense signal from the metal ion and weak or undetectable signals from the intact metal-containing molecular species.[12,21,38]

In the 24 390 cm^{-1} spectrum, the fragmentation pattern is similar to that observed in the mass spectrum at 21 170 cm^{-1}. However, the relative intensities of the metal-containing molecular fragments have noticeably increased from the spectra at lower energies. Both the molecular ion and the monoligated fragment intensities have increased by a factor of 20 compared to those in the spectrum obtained at 21 170 cm^{-1}. The molecular ion intensity is now greater than the intensity of the metal ion. The presence of a molecular ion signal implies that ionization of chromocene occurs before the molecule dissociates. Fragmentation of the ionized molecule may then occur by sequential ligand loss until Cr$^+$ is produced. This mechanism is also supported by the presence of the intense signals from the monoligated and the free ligand ions.

The intensities of the C$_n^+$ cyclopentadienyl fragments are similar at the energies discussed so far but the increase in intensity of the Cr(C$_3$H$_3$)$^+$ and CrC$_2^+$ fragments may be a direct result of the increased amount of the corresponding monoligated species formed during the photodissociation process. The metal atom may be bonded to the cyclopentadienyl moiety in an allyl-like fashion after excitation. The formation of Cr(C$_3$H$_3$)$^+$ and CrC$_2^+$ then suggests an intramolecular process by which the cyclopentadienyl ring of the monoligated species fragments to leave behind allyl- and ethylene-like bonded fragments. To the best of our knowledge, this is the first reported photon driven fragmentation mechanism that is so characteristically sequential.

2. Correlation of the Photofragmentation with Resonant Electronic Excited States. The REMPI spectra obtained by monitoring Cr(Cp)$_2^+$, Cr(Cp)$^+$, and Cr$^+$ demonstrate the wavelength dependence of the photofragmentation as shown in Figure 2a, 2b, and 2c, respectively. Interestingly, the wavenumber region where the Cr(Cp)$_2^+$ signal increases dramatically (∼23 530 cm^{-1}) is the same as that where the Cr$^+$ signal decreases. The relative intensities of the Cr(Cp)$_2^+$ to Cr$^+$ ions in the REMPI spectra are related to the electronic absorption bands of the molecule.[39] A ligand-to-metal charge transfer (LMCT) band has been reported at the high energy region of the REMPI spectra. A metal centered d−d band has been reported in the 22 500−23 500 cm^{-1} region where the Cr$^+$ ion peak is dominant.

A. Excited States of Chromocene. The electronic absorption spectra in the UV/vis region has been reported for chromocene in isooctane[39] solution and in a frozen argon matrix.[40] Similar spectral features were observed in both of the media. The lowest energy peak maximum occurs at 21 970 cm^{-1}, has an extinction coefficient of 186 M^{-1}cm^{-1} and originates from ^{3}E$_2'$ → ^{3}E$_1'$, ^{3}E$_2'$, ^{3}A$_1'$, ^{3}A$_2'$ transitions.[39] The ligand-to-metal charge-transfer transition at 29 590 cm^{-1} has an extinction coefficient of 2700 M^{-1} cm^{-1} and is assigned to the ^{3}E$_2'$ → ^{3}E$_1''$ transition.[39]
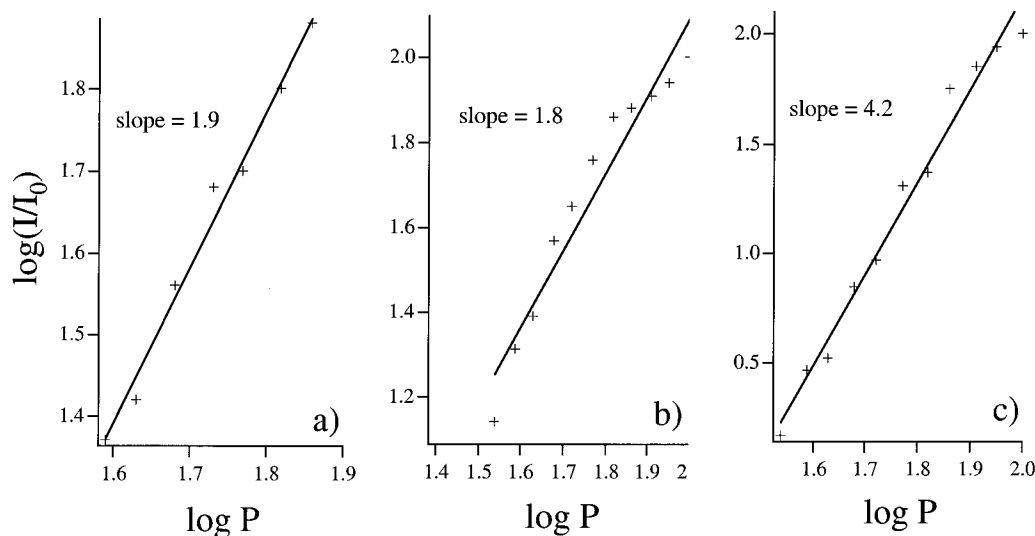
Figure 4. log−log plots showing the power dependencies for the molecular ion and metal ion at various wavelengths. The slope of the line gives the observed photon dependence. (a) Photon dependence for the molecular ion using 24 260 cm^{-1} excitation. (b) Photon dependence for the metal ion using 24 320 cm^{-1} excitation. (c) Photon dependence for the metal ion using 23 490 cm^{-1} excitation.

The gas-phase structure of chromocene has eclipsed cyclopentadienyl rings (D_{5h} symmetry).[41] The ground state of chromocene is $^3E_2'$ with an electron configuration of $(a_1')^1(e_2')^3$.[41−43] Two other orbitals will play a role in the following discussion. The lowest energy completely unoccupied molecular orbital is e_1'' and the highest energy completely occupied orbital is e_1'.

The band maximum of the lowest energy spin allowed d−d transition is observed at 22 000 cm^{-1} in isooctane and at 23 000 cm^{-1} in a frozen argon matrix.[40] The band involves a group of transitions from either the a_1' or e_2' to the e_1'' orbital.[44] The a_1 orbital is primarily metal d_z^2 in character and the e_2 orbitals are primarily metal d_{xy} and $d_{x^2-y^2}$ in character. The lowest empty orbital, e_1'', is the antibonding combination of the metal d_{xz} and d_{yz} orbitals with the e_1' π-orbitals of the ring.[45] This molecular orbital is sketched on the left side of Figure 5. The band maximum of the lowest energy charge-transfer band is observed at 29 590 cm^{-1} in isooctane. The transition is from the $1e_1'$ orbital to the e_2' orbital.[39] The $1e_1'$ orbital is predominantly ligand in character, and the transition is characterized as a ligand to metal charge transfer.

B. Bonding Changes in Excited States and Photofragmentation. The bonding and antibonding changes that occur when the d−d and charge-transfer excited states are populated by absorption of the first photon provide a simple explanation for the photofragmentation processes that occur. These processes and the excited states involved are shown in Figure 5.

When the excitation energy is in resonance with the d−d excited state of chromocene, the first photon populates the d−d state. The promotion of an electron from the a_1' or e_2' orbital to the antibonding e_1'' orbital will weaken the M−Cp bond.[41] The second photon is absorbed by the weakened molecule and causes fragmentation. It cannot cause ionization because the ionization potential of chromocene is 44 362 cm^{-1}.[43] Thus, fragmentation before ionization is the dominant pathway and Cr$^+$ dominates the mass spectra. The resonance peaks in the REMPI spectra show that ligand dissociation to form a neutral chromium atom is a favored pathway in this region and that dissociation events occur prior to molecular ionization. The fragments produced from this state include the neutral chromium atom (as indicated by the resonances) and ligand fragments. Subsequent photon absorption ionizes these fragments. The intact parent molecule
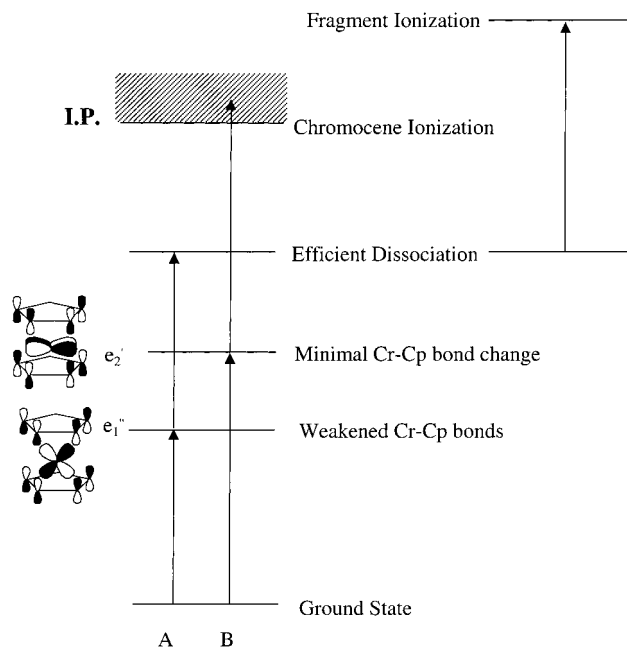

Figure 5. Electronic energy diagram for chromocene with D_{5h} symmetry. The probability contours of the e_1'' and e_2' molecular orbitals are sketched on the left. The possible processes arising from multiphoton absorption and a proposed explanation for the photofragmentation processes are shown to the right of the different excited states involved. The arrows above A represent the processes when the first photon is in resonance with the d−d state, and the arrows above B represent the processes when the first photon is in resonance with the LMCT state.

peaks are at a minimum, probably because the parent cannot remain intact long enough to be ionized and observed.

In contrast, when the excitation is in resonance with the charge transfer state, little bond weakening occurs. The one-electron transition promotes an electron from an orbital that is primarily localized on the ligand to one that is primarily metal d orbital in character and slightly metal−ligand bonding. The second photon is absorbed by a molecule that has metal−ligand bonds relatively unchanged from that of the ground-state molecule; fragmentation is minimal. In addition, the combined energy of the two photons is above the ionization potential of the molecule. Thus, ionization of the intact molecule is an important photoprocess and the most intense peak in the mass
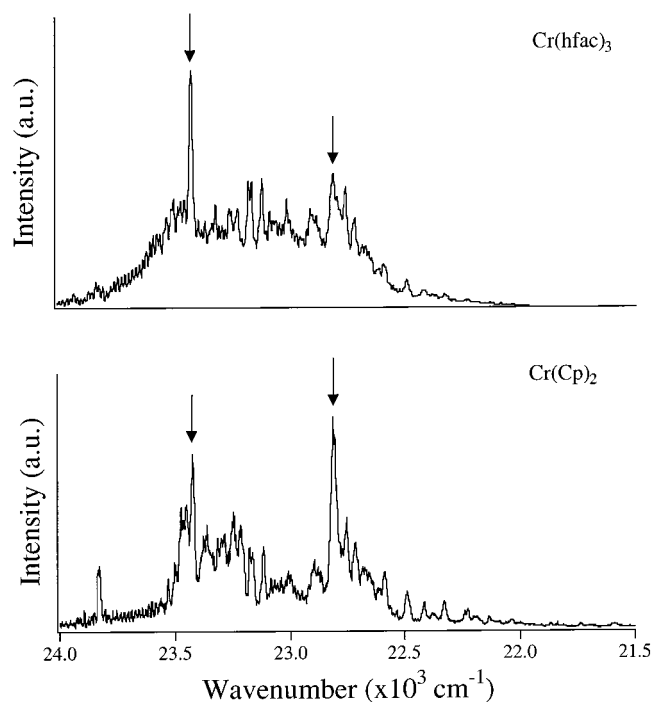
Figure 6. REMPI spectra monitoring the Cr^+ signal resulting from excitation of (a) $Cr(hfac)_3$ and (b) $Cr(Cp)_2$. The two sharp peaks appearing in both spectra at 23 430 and 22 810 cm^{-1} have been previously assigned to Cr atom transitions.

spectrum is that from the parent ion. However, fragmentation also occurs; the intensity of the $Cr(Cp)^+$ ion is about one-half that of the molecular ion, and chromium ion intensity is slightly less than that of the parent ion.

It is important to note that in each region both the Cr^+ and the $Cr(Cp)_2^+$ ions are always observed, but the intensities of the fragments fluctuate dramatically within each band. The presence of both ions is understandable because there is overlap between the absorption bands of the molecule.

3. Chromium Atom Resonances. The REMPI spectra that are obtained by monitoring the chromium ion contain sharp peaks. These peaks are observed in all of the wavelength regions that are studied. In addition, sharp losses of intensity or "dips" at the same wavenumber as the peaks are observed in some of the REMPI spectra obtained by monitoring the parent ion or the mono-ligated fragment.

The sharp peaks in the spectra that are obtained when Cr^+ is monitored (Figure 2c) are assigned to atomic resonances of neutral Cr and possibly to atom-like absorptions by a molecule in an excited state in which the metal atom is very weakly associated with the ligand. The assignment of most of these sharp peaks to atomic resonances of neutral Cr is further confirmed by comparing the REMPI spectra obtained monitoring Cr^+ to that obtained from the photolysis of a different chromium-containing molecule, $Cr(hfac)_3$. The spectrum obtained from $Cr(hfac)_3$ is compared to that from chromocene in Figure 6. There are many peaks in common in the two spectra, supporting the assignment of the peaks to Cr atom resonances. The two most intense peaks at 23 430 and 22 810 cm^{-1} have previously been assigned to Cr atom transitions[46] and are due to the $^3H^°_6$ (4p) $\rightarrow$ $^3G_5$ (4s) and $^5F^°_4$ (4p) $\rightarrow$ $^5D_4$ (4s^2) transitions.

Careful inspection of Figure 6 at 23 830 cm^{-1} shows a dip in the $Cr(Cp)_2^+$ spectrum that corresponds to a peak in the Cr^+ spectrum. The effect on the intensities of fragments observed in the mass spectra when the excitation is off and on a Cr resonance is shown in Figure 3a and 3b, respectively. Two

possible explanations for this behavior are (a) inner filter effects that decrease the amount of photons available for $Cr(Cp)_2$ ionization after Cr has absorbed photons and (b) neutralization of chromocene ions by electrons released from chromium atoms. Absorption of photons by the metal atom at resonant frequencies may be so efficient that the number of photons available for other photoprocesses such as forming the molecular ion may not be sufficiently large. Another possibility is that during resonant ionization of neutral Cr atoms, the electrons that are produced are captured by positively charged fragments. The result would be the neutralization of these ions rendering them undetectable by mass spectroscopy.

Summary

The gas phase laser photochemistry of chromocene is strongly wavelength dependent. The most important photoproduct that is detected by mass spectroscopy when the molecule is irradiated at energies less than about 23 530 cm^{-1} is the Cr^+ ion. The REMPI spectrum contains numerous intense sharp lines in the region between 22 000 and 23 530 cm^{-1} and a relatively featureless broad band at lower energies. Surprisingly, in the region greater than 23 530 cm^{-1}, the most prominent photoproduct is the $Cr(Cp)_2^+$ ion. This result is in contrast to the multiphoton ionization mass spectroscopic results of all of the other metallocenes that have been studied to date where the metal ion always dominates. The maximum reported ratio of intact metallocene ion to metal ion is 0.005 to 1 for nickelocene. In the case of chromocene, the maximum ratio in the wavelength region studied is 1.3 to 1 at 24 390 cm^{-1} excitation. The wavelength dependence is correlated with both the bonding changes that occur in the initially populated excited states and the ionization energy of the molecule. When the initially populated state is the ligand to metal charge transfer state, the first photon causes minimal bond weakening and the second photon excites the intact molecule above the ionization continuum, resulting in efficient ionization of the parent molecule. When the initially populated state is a lower energy ligand field state, significant bond weakening occurs and absorption of a second photon results in significant photodissociation prior to ionization producing intense fragment peaks dominated by the metal ion peak. The intensity ratio of the parent ion to chromium ion in this case never exceeds 0.16:1. The sharp lines in the REMPI spectrum that are observed when the Cr^+ ion is monitored are assigned to chromium atom resonances. Sharp dips that are observed in the REMPI spectra when other ions are monitored are attributed to either a type of inner filter effect or to electron capture by the other ions.

References and Notes

(1) Morosanu, C. E. *Thin Films by Chemical Vapor Deposition*; Elsevier: New York, 1990.

(2) Eden, J. G. *Photochemical Vapor Deposition*; Wiley: New York, 1992.

(3) Hitchman, M. L.; Jensen, K. F. *Chemical Vapor Deposition: Principles and Applications*; Academic Press: San Diego, 1993.

(4) Kodas, T. T.; Hampden-Smith, M. J. *The Chemistry of Metal CVD*; Weinheim: New York, 1994.

(5) Braichotte, D.; Garrido, C.; van den Bergh, H. *Appl. Surf. Sci.* **1990**, *46*, 9−18.

(6) Cheon, J.; Talaga, D. S.; Zink, J. I. *Chem. Mater.* **1997**, *9*, 1208−1212.

(7) Cheon, J.; Talaga, D. S.; Zink, J. I. *J. Am. Chem. Soc.* **1997**, *119*, 163−168.

Photooxidation vs Photofragmentation of Chromocene

J. Phys. Chem. A, Vol. 105, No. 38, 2001 **8671**

(8) Jackson, R. L. *Acc. Chem. Res.* **1992**, *25*, 581−586.

(9) Smalley, R. E.; Wharton, L.; Levy, D. H. *Acc. Chem. Res.* **1977**, *10*, 139−145.

(10) Willwohl, H.; Wolfrum, J. *Appl. Surf. Sci.* **1992**, *54*, 89−94.

(11) Cheon, J.; Guile, M.; Muraoka, P.; Zink, J. I. *Inorg. Chem.* **1999**, *38*, 2238−2239.

(12) Muraoka, P.; Byun, D.; Zink, J. I. *J. Am. Chem. Soc.* **2000**, *122*, 1227−1228.

(13) Cheon, J.; Zink, J. I. *J. Am. Chem. Soc.* **1997**, *119*, 3838−3839.

(14) Talaga, D. S.; Hanna, S. D.; Zink, J. I. *Inorg. Chem.* **1998**, *37*, 2880−2887.

(15) Talaga, D. S.; Zink, J. I. *Inorg. Chem.* **1996**, *35*, 5050−5054.

(16) Bar, R.; Heinis, T.; Nager, C.; Jungen, M. *Chem. Phys. Lett.* **1982**, *91*, 440−442.

(17) Braun, J. E.; Neusser, H. J.; Harter, P.; Stockl, M. *J. Phys. Chem. A* **2000**, *104*, 2013−2019.

(18) Engelking, P. C. *Chem. Phys. Lett.* **1980**, *74*, 207−210.

(19) Leutwyler, S.; Even, U.; Jortner, J. *Chem. Phys. Lett.* **1980**, *74*, 11−14.

(20) Leutwyler, S.; Even, U.; Jortner, J. *Chem. Phys.* **1981**, *58*, 409−421.

(21) Leutwyler, S.; Even, U.; Jortner, J. *J. Phys. Chem.* **1981**, *85*, 3026−3029.

(22) Liou, H. T.; Engelking, P. C.; Ono, Y.; Moseley, J. T. *J. Phys. Chem.* **1986**, *90*, 2892−2896.

(23) Liou, H. T.; Ono, Y.; Engelking, P. C.; Moseley, J. T. *J. Phys. Chem.* **1986**, *90*, 2888−2892.

(24) Nagano, Y.; Achiba, Y.; Kimura, K. *J. Phys. Chem.* **1986**, *90*, 1288−1293.

(25) Niles, S.; Prinslow, D. A.; Wight, C. A.; Armentrout, P. B. *J. Chem. Phys.* **1992**, *97*, 3115−3125.

(26) Opitz, J.; Harter, P. *Int. J. Mass Spectrom. Ion Processes* **1992**, *121*, 183−199.

(27) Ray, U.; Hou, H. Q.; Zhang, Z.; Schwarz, W.; Vernon, M. *J. Chem. Phys.* **1989**, *90*, 4248−4257.

(28) Tyndall, G. W.; Larson, C. E.; Jackson, R. L. *J. Phys. Chem.* **1989**, *93*, 5508−5515.

(29) Lubman, D. M.; Jordan, R. M. *Rev. Sci. Instrum.* **1985**, *56*, 373−376.

(30) Wiley: W. C.; McLaren, I. H. *Rev. Sci. Instrum.* **1955**, *26*, 1150−1157.

(31) Gedanken, A.; Robin, M. B.; Kuebler, N. A. *J. Phys. Chem.* **1982**, *86*, 4096−4107.

(32) Johnson, P. M. *Acc. Chem. Res.* **1980**, *13*, 20−26.

(33) Antonov, V. S.; Letokhov, V. S. *Appl. Phys.* **1981**, *24*, 89−106.

(34) Ashfold, M. N. R.; Howe, J. D. *Annu. Rev. Phys. Chem.* **1994**, *45*, 57−82.

(35) Lubman, D. M.; Kronick, M. N. *Anal. Chem.* **1982**, *54*, 660−665.

(36) Ashfold, M. N. R.; Clement, S. G.; Howe, J. D.; Western, C. M. *J. Chem. Soc., Faraday Trans.* **1993**, *89*, 1153−1172.

(37) Schlag, E. W.; Neusser, H. J. *Acc. Chem. Res.* **1983**, *16*, 355−360.

(38) Mikami, N.; Ohki, R.; Kido, H. *Chem. Phys.* **1990**, *141*, 431−440.

(39) Gordon, K. R.; Warren, K. *Inorg. Chem.* **1978**, *17*, 987−994.

(40) Chetwynd-Talbot, J.; Grebenik, P.; Perutz, R. N. *Inorg. Chem.* **1982**, *21*, 2647−2657.

(41) Gard, E.; Haaland, A.; Povak, D. P.; RSeip, R. *J. Organomet. Chem.* **1975**, *88*, 181−189.

(42) Evans, S.; Green, M. L. H.; Jewitt, B.; King, G. H.; Orchard, A. F. *J. Chem. Soc., Faraday Trans. 2* **1974**, *70*, 356−376.

(43) Rabalais, J. W.; Werme, L. O.; Bergmark, T.; Karlsson, L.; Hussain, M.; Siegbahn, K. *J. Chem. Phys.* **1972**, *57*, 1185−1192.

(44) Warren, K. D. *Inorg. Chem.* **1974**, *13*, 1243−1246.

(45) Brennan, J.; Cooper, G.; Green, J. C.; Payne, M. P.; Redfern, C. M. *J. Elect. Spec. Relat. Phenom.* **1993**, *66*, 101−115.

(46) Meggers, W. F.; Corliss, C. H.; Scribner, B. F. *Tables of Spectral-Line Intensities*; National Bureau of Standards: Washington, 1975.